International Biodeterioration & Biodegradation 83 (2013) 56–62

Contents lists available at SciVerse ScienceDirect

International Biodeterioration & Biodegradation

journal homepage: www.elsevier.com/locate/ibiod

Colocalizing incipient reactions in wood degraded by the brown rot fungus *Postia placenta*

Jonathan S. Schilling [a,*], Shona M. Duncan [a,1], Gerald N. Presley [a], Timothy R. Filley [b], Joel A. Jurgens [c,2], Robert A. Blanchette [c]

[a] Department of Bioproducts and Biosystems Engineering, University of Minnesota, 108 Kaufert Laboratory, 2004 Folwell Avenue, Saint Paul, MN 55108, USA
[b] Department of Earth and Atmospheric Sciences and the Purdue Climate Change Research Center, Purdue University, 550 Stadium Mall Drive, West Lafayette, IN 47907, USA
[c] Department of Plant Pathology, University of Minnesota, 1991 Upper Buford Circle, Saint Paul, MN 55108, USA

ARTICLE INFO

Article history:
Received 13 March 2013
Received in revised form
8 April 2013
Accepted 9 April 2013
Available online

Keywords:
Fenton
Brown rot
Decay
GH61
Polysaccharide monooxygenase
Glycosyl hydrolase

ABSTRACT

Brown rot fungi are theorized to use both free radicals and enzymes to degrade wood. If these incompatible agents are employed in sequence (enzymatic after oxidative) in order to avoid interaction, this should be resolvable spatially in rotting wood. To assess this, we used thin spruce wafers as substrates, with the largest face the transverse plane. Propped wafers were colonized from the bottom (tangential to grain) by *Postia placenta*, using wood cell orientation and gravity to slow fungal egress and accentuate spatial gradients. After brief colonization, wafers were cut into 1-mm strips progressing up the wafer, and subsectioned for complementary analyses. Analyses included fungal growth, pH, cellulase activity, and wood modifications attributable to non-enzymatic mechanisms. Hyphae were imaged using confocal microscopy of fluorophore-tagged chitin. Dilute alkali solubility and lignin demethylation were measured as proxies (consequences) of carbohydrate depolymerization and lignin oxidation, respectively. Because *P. placenta* lacks genes for cellobiohydrolases, endoglucanase (EG) activity was measured. In composites of reassembled sections, hyphal fronts and apparent depolymerization preceded EG and lignin demethylation fronts by more than 6 mm. Although detection limits are a caveat when implicating novel fungal metabolites, results encourage and provide methodology for targeting this interesting leading edge of cellulolysis.

1. Introduction

The mechanisms that brown rot fungi use to degrade lignocellulose remain unclear, and better characterization of this metabolic system is valuable. The biological transformations of plant tissues during brown rot complement those desired during industrial conversion following the biochemical platform (Saha, 2004; Schilling et al., 2012). These fungi effectively overcome the lignin barrier in plant cell walls without removing significant amounts of lignin, and mimicking this industrially would save lignin as a by-product. These fungi are also ubiquitous wood-degrading organisms in forests and are common pests in buildings (Gilbertson and Ryvarden, 1986). Wood metabolized by brown rot fungi becomes rich in lignin as cellulose and hemicellulose are removed preferentially (Eriksson et al., 1990). In contrast with white rot, when lignin is more extensively mineralized, brown rot yields lignin residues with longer forest floor residence times and unique biogeochemical attributes (Rypáček and Rypáčková, 1975; Jurgenson et al., 1977; Gilbertson, 1980; Zabel and Morrell, 1992; Filley et al., 2002; Song et al., 2012).

Brown rot fungi are theorized to use a two-step mechanism when degrading wood cells, but partition these reactions away from each other and at an undetermined distance from the fungus. The initial step has, by far, received the most research focus as it severely reduces strength prior to a significant loss of wood mass (Winandy and Morrell, 1993). Only recently has there been increased focus on cellulolytic enzymes among the multiple lineages of brown rot fungi, with emerging interest in ill-defined enzymes (e.g., GH61 family) that may assist in cellulolysis (Žifčáková and Baldrian, 2012). With the traditional assumption of

* Corresponding author. Tel.: +1 612 624 1761; fax: +1 612 625 6286.
E-mail addresses: schillin@umn.edu (J.S. Schilling), presl034@umn.edu (G.N. Presley), filley@purdue.edu (T.R. Filley), robertb@umn.edu (R.A. Blanchette).
[1] Present address: Wisconsin Institute for Sustainable Technology, University of Wisconsin-Stevens Point, Stevens Point, WI 54481, USA.
[2] Present address: Sustainable Provision of Ecosystem Services Project, Flora and Fauna International, Phnom Penh, Cambodia.

0964-8305/$ – see front matter © 2013 Elsevier Ltd. All rights reserved.
http://dx.doi.org/10.1016/j.ibiod.2013.04.006

endoglucanase-dependent cellulolysis during brown rot, theories generally provide for partitioning of Fenton-based reactions from cellulases in three steps. 1) In a single wood cell, low-molecular weight fungal agents diffuse from the wood cell lumen, where the fungus resides, across the S3 layer and into the S2 layer of the wood secondary wall (Hyde and Wood, 1997; Goodell et al., 1997; Kerem et al., 1998). 2) These agents, including a source for hydrogen peroxide, collaborate to reduce iron and drive the Fenton reaction, producing highly reactive hydroxyl radicals (HO•). 3) Radicals react with the plant cell wall at a distance from hyphae and from endoglucanases too large to penetrate the S3 layer (Fluornoy et al., 1991; Srebotnik and Messner, 1991).

In wood, there are predictable changes that are attributed to the Fenton-based step. Oxalic acid secretion, acidification (Espejo and Agosin, 1991; Schilling and Jellison, 2005), and a significant increase in the alkali solubility of residues are all characteristic of brown rot, the latter believed to be distinct from white rot due to rapid, endo-acting depolymerization of holocellulose (Campbell, 1952; Cowling, 1961; ASTM, 2007; Shortle et al., 2010). Carbohydrates are removed selectively, often starting with side chain hemicelluloses (Curling et al., 2002), while less (wt%) of the lignin fraction is degraded. These lignin losses occur, at least in part, due to demethylation of lignin (Kirk, 1975; Filley, 2003), a modification that is a signature of brown rot and that has been attributed to the action of reactive oxygen species such as the hydroxyl radical (Filley et al., 2002). Assuming these observable consequences can be directly attributed to or implicated with the initial oxidative step in brown rot, these should be spatially resolved from both the fungal hyphae and the endoglucanase (EG) assumed to be the main cellulase in most brown rot secretomes (Martinez et al., 2009; Floudas et al., 2012).

In this study, our goal was to spatially map wood as it was degraded by a brown rot fungus, colocalizing incipient tissue modifications with hyphae and extracellular EG activity. The words 'at a distance' have been used prolifically in the literature, including our own (Schilling and Bissonnette, 2008), to describe the spatial separation of brown rot Fenton-based reactions from hyphae, but the scale of separation is unclear. Although the low-molecular weight system has generally been described across single wood cell walls, the advance of strength loss relative to colonization suggests that oxidative reactions might occur at much larger distances away from hyphae. Determining this distance has bearing both on diagnostics of lumber defects and on consolidated bioprocessing of wood chips. A spatially-resolved experimental set-up can also allow assessment of temporal patterns, tracking the sequence as fungi progressively unlock carbohydrates from lignocellulose, and these endeavors can now utilize a growing wealth of annotated fungal genomes to incorporate transcriptomics (Martinez et al., 2009; Eastwood et al., 2011; Floudas et al., 2012).

Our approach was to use thin wood wafers to encourage gradients relative to the hyphal front, exploiting a low-porosity wood species, cross-grain wood orientation, and gravity, and then sectioning and overlaying results. Specifically, we chose *Postia placenta* as a model brown rot fungus with an annotated genome and a history of physiological research.

2. Methods

2.1. Decay chambers

30 ml of 2% malt extract agar was solidified in pint jars and inoculated with a 1-cm^2 plug of a 14-day culture of *P. placenta* (isolate MAD 698-R). A sterilized circular mesh (co-polymer Gutter Guard, Amerimax, PA, USA) cut to fit the jars was laid flat on the agar. At the point of full mycelial coverage of the medium (2–4 weeks), spruce wafers were added, propped vertically against the sides of the jars. Up to four wafers were added per jar. Wafers (7-cm length) were cut from untreated spruce lumber into 7-mm thick wafers, the largest plane being transverse (23-mm width) (Fig. 1). Wafers were oven-dried (100 °C, 48 h) and weighed prior to steam sterilization and addition to microcosms, with the radial plane side resting on the mycelium. A second set of wafers (6-cm length) used for targeted testing with replication ($n = 3$ per section, per analysis) were pre-soaked in distilled water under vacuum for three minutes prior to sterilization and developed decay faster than those without a pre-soak (Fig. 1). The wafer design forced hyphae to grow across the grain but not across annual rings, minimizing variability and maximizing cell-to-cell gradients.

2.2. Wafer processing

Wood was sectioned, analyzed, and reassembled to create a composite image, similar to building a panorama from a progressive series of pictures. At harvest, the distance of visible fungal growth up the wafers was recorded, and hyphae were scraped from the surfaces. Strips (strips = vertical cuts) were carefully cut from fresh wafers over the length from the bottom to the top using a razor and a vice as a straight edge (Fig. 1). Fresh strips were sectioned (sections = horizontal cuts) at 1-mm intervals, with one set analyzed for EG activity and the other frozen in cryo-protectant at −80 °C for microscopy. The remaining large strip was stored at −80 °C until sectioning, oven-drying and grinding to 40 mesh in a Wiley mill for wood modification analyses. Unlike 1-cm sections for other analyses, dilute alkali solubility (DAS) was measured on 2-mm sections in order to yield enough material for the test.

2.3. Hyphal localization

Hyphal distance vertically up the wafers was recorded for each sampled wafer and generally was uniform as a horizontal front moving up the wafer. The visible hyphal front was matched by analysis of hyphal progress within wood cells by fluorescent staining of chitin. Cryotomed radial sections (100 μm thick) were

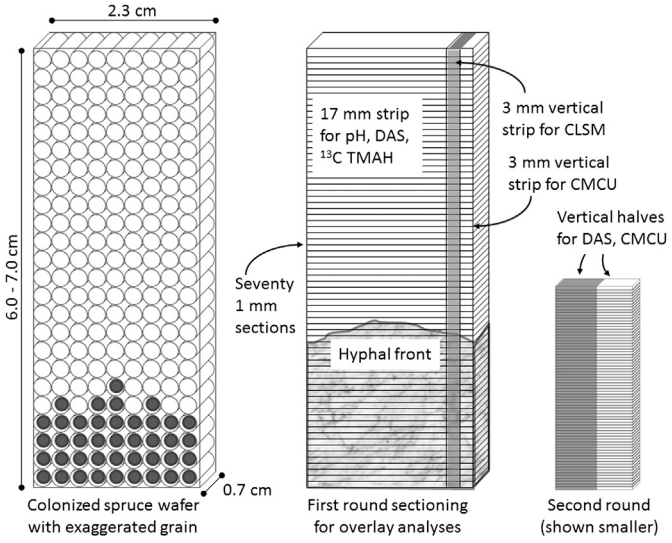

Fig. 1. Schematic of set-up for two experiments, one with a suite of analyses and a second targeting two key characters. Spruce wafers (left, showing grain angle) were added to soil-block jars with the smallest plane (radial) in contact with developed mycelia of *Postia placenta*. The round one wafers were harvested at 14 days ($n = 40$). The wafers from the round two trial were harvested at day 14, 18, or 21 ($n = 24$). Wafers were sectioned and subsectioned for analyses as shown, using pre-moistened wood and larger sample sections for round two.

made at intervals progressing up the wafers. Wood was infiltrated with a non-crystal forming Tissue Freezing Medium™ (Triangle Biomedical Sciences, Durham, NC, USA) and sectioned to approximately 100 μm with an OM 2488 MinotomeR microtome-crystat (International Equipment Company, Needham Heights, MA, USA) at −20 °C. Sections were mounted on treated glass slides to help with adhesion, hydrated with pH 7.4 phosphate buffered saline (PBS) for 10 min and dyed for 10 min with wheat germ agglutinin, tetramethylrhodamine conjugate (10 mg ml^{-1}) (Invitrogen, USA). PBS-rinsed sections were viewed on a Nikon C1 Spectral Imaging Confocal Laser Scanning Microscope (CLSM). The 488 and 567 laser bands were used to excite and separate the wood tissue from fungal hyphae, and similar ranges were used for detection.

2.4. Enzyme localization

For cellulase activity, sections cut from the fresh EG strip were added per well to a 96-well microtiter plate for enzyme extraction and analyzed using a 1/10th scale Azo-carboxymethylcellulose (CMC) EG assay method as per manufacturer's instructions (Megazyme, Bray, Ireland). Wells were parafilm-sealed and incubated at 40 °C and 120 rpm in 50 μl sodium acetate buffer (100 mM, pH 4.6) for 3 h. Azo-CMC was then added and the plate returned to 40 °C for 30 min, or for 10 min in the second round extracting from larger wafer sections. The reaction was stopped and the samples vortexed, centrifuged, and supernatant absorbance analyzed at 590 nm following the Azo-CMC manufacturer guidelines. Activity was expressed as CMC units (CMCU) per 1-mm wood section, without correcting for protein concentration in order to focus on overall activity and not per-enzyme potential. Hemicellulase activities of xylanase, mannanase, galactanase were measured using Azo-dyed substrates and parallel protocols.

2.5. Wood modification analyses

Wood pH, DAS, and lignin demethylation were measured from ground, oven-dried powder. The pH and DAS were from single sections and were measured following detailed protocols (Shortle et al., 2010). Lignin modifications required sample pooling, described in the next paragraph, and were analyzed using ^{13}C-labeled tetramethylammonium hydroxide (TMAH) thermochemolysis, following methods described previously (Filley et al., 2006; Schilling et al., 2012). Past experiments have shown that during brown rot, the relative proportion of permethylated vanillic acid to vanillin ratio, often termed acid to aldehyde (Ac/Al) or G4/G6, increases progressively over the course of decay (Filley et al., 2002). In previous work (Schilling et al., 2012), the most sensitive lignin modification to brown rot was the increase in G4 demethylation residues, possibly attributed to oxidative alteration of the alpha carbon on lignin's propanoid chain to yield vanillic acid during TMAH thermochemolysis.

The sample size required for TMAH thermochemolysis was too large for the sections taken from individual wafers. To compensate for this issue without compromising resolution, the EG distance up the wafer, which varied from wafer to wafer, was used as a benchmark. Because EG activity showed an abrupt transition in many of the wafer samples, this was set as the 'EG front'. TMAH was then used to analyze pooled samples from sections extending beyond this front. For example, if one wafer had an EG front at 15 mm and another wafer had the EG front at 20 mm, we would pool the 16 and 21 mm sections, respectively, as '1 mm past EG front' samples. Fourteen wafers with clear and abrupt EG fronts were pooled for TMAH, and samples were analyzed at the point of fungal ingress into the wafer base and extending 6 mm from the EG front.

2.6. Colocalization

A sharp EG front refined our analyses to 14 wafers for colocalization efforts. In these select wafers, we overlay hyphal fronts (visually observed and via confocal microscopy) for individual wafers and overlay pH and DAS measures as matched data per wafer. The pooled thermochemolysis data was used to infer the extent of oxidative lignin modification at the wafer base and up to 6 mm ahead of the EG front, as a mean value to be colocalized using the EG front as a baseline among wafers.

3. Results

Using thin wood substrates resulted in 35% of wafers having uniform and abrupt EG fronts amenable to fine-scale colocalization. The zone of elongation for the mycelial front inside the wood wafers showed a gradual increase in hyphal density but was abrupt and slightly more advanced on wafer surfaces (Fig. 2). This clear hyphal front, visible to the eye, allows one to easily target the zones of interest evolving inside the wafers. Only in rare instances were hyphae seen colonizing isolated wood cells ahead of the mycelial front, but variability across some wafers (horizontally) may have caused some wafers to have non-uniform enzyme fronts. The 14 wafers with abrupt EG fronts were used for pooled TMAH analyses,

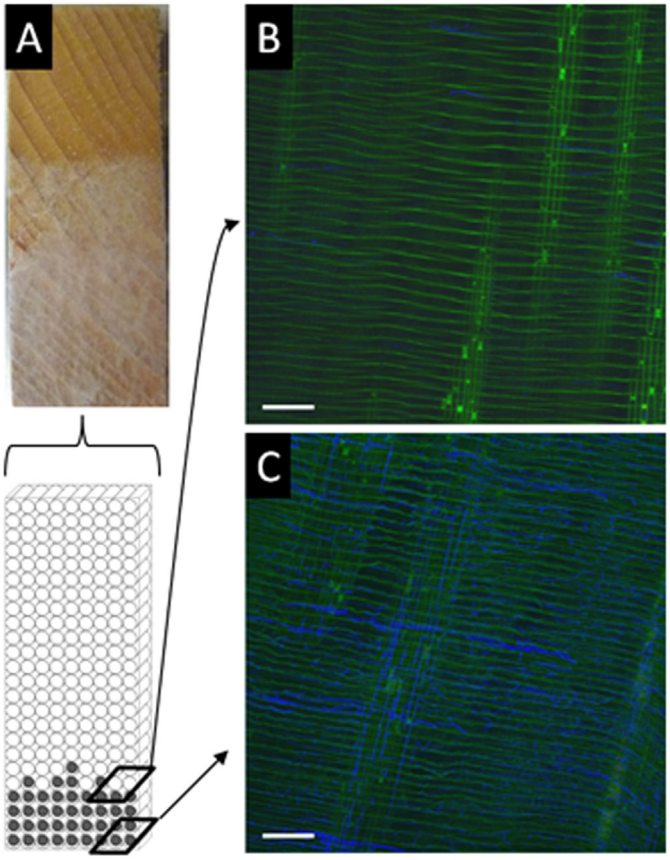

Fig. 2. Hyphal front visualizations using the eye and confocal microscopy, with chitin-stained fungal hyphae (blue) in wood cells (green). Growing against the grain, *P. placenta* formed an abrupt front visible to the eye (A). Using a single wafer (#29) to colocalize, progress toward a front inside of wood was more gradual, yielding nearly 100% wood cell lumen occupation near the colonization point at 1 mm (B) and lower occupation near the front at 18 mm (C), relative to a visible front at 22 mm. Though not shown, hyphae commonly traveled through bordered pits, demonstrating growth cell-to-cell inside the wafer. Scale bar = 100 μm. (For interpretation of the references to colour in this figure legend, the reader is referred to the web version of this article.)

and 2 outstanding samples were used further to characterize pH and for CLSM imaging. The second wafer trial, using pre-soaked wafers and providing larger amounts of sample material for analyses, yielded more progressed hyphal fronts, less variable EG results, and more defined EG fronts.

The hyphal progress and a correlated drop in pH clearly preceded detectable EG activity inside the wood. The EG front in most cases in the first round trials was pronounced and close to the point of colonization (Fig. 3A). The pH progressing from the same point of colonization indicated acidification at distances ahead of the EG front and mirroring the hyphal progress inside the wood (Fig. 3B). Fig. 3A shows the low levels of a main-chain specific enzyme, xylanase, in a single wafer, and similar results were found for galactanase and mannanase, two enzymes relevant to conifer wood degradation.

To probe the coincident lignin modifications, pooled wafer samples adjusted to reflect the proximity to the EG front were analyzed with a focus on the G4 and G6 residues. These residues showed significant demethylation coincident with areas of high EG activity, but beyond the EG front, demethylation levels were not statistically different from those in non-degraded control wood (Fig. 4). This was true for both G4 and G6, which showed similar patterns and indicated that demethylation and EG secretion, at least as detectable, were coincident and not staggered.

Both lignin demethylation and EG activity lagged behind the progress of the mycelial front and, surprisingly, behind an advance in detectable depolymerization using DAS (Fig. 5A). Where the hyphal front had advanced nearly the entire distance of the wafer, the apparent EG activity per section depressed at distances behind the front (Fig. 5B). In correlating DAS with EG in this wafer (Fig. 6A), DAS preceded the EG front by approximately four sections, representing 8 mm or nearly 20% of the total colonization progress of the fungus. A similar pattern was present when combining data from wafers colonized three weeks (Fig. 6B, $n = 3$). These results show coincident, not staggered reactions, but localize both behind the advancing progress of hyphae and acidification of the wood, as well as the process of carbohydrate depolymerization.

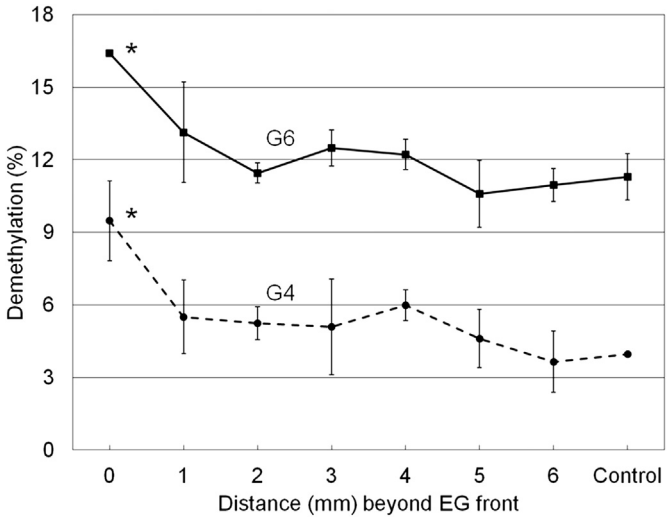

Fig. 4. Lignin demethylation in samples pooled as a function of proximity to the EG front. Demethylation in G4 and G6 residues, measured by ^{13}C TMAH, was significantly (denoted by *) elevated relative to the control but also to residues extending at a distance beyond the cellulase front, suggesting coincident not staggered enzymatic/oxidative reactions. Analysis of variance with post-hoc Tukey's means comparisons was used with alpha of 0.05. Error bars are standard deviations.

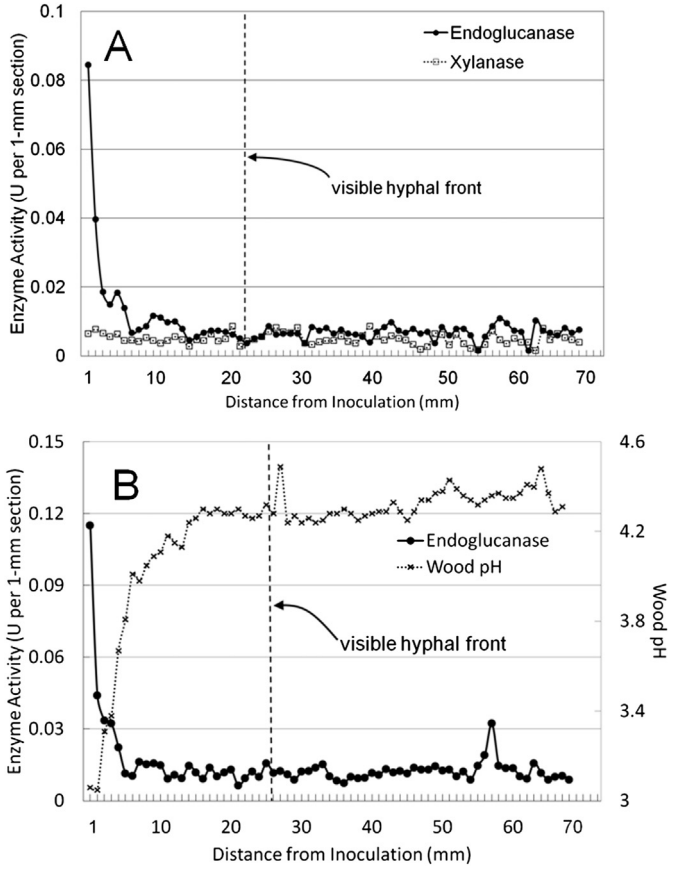

Fig. 3. Cellulolytic activity in wood as a function of distance from the point of colonization (wafer base) by *P. placenta*. Focusing on the same wafer (#29) presented in Fig. 2, endoglucanase (EG) activity peak was close to the point of colonization and behind progressing hyphae (A). In a separate wafer (#19), pH was gradually depressed extending back from the visible hyphal front on the wafer surface (B). At a given distance from the point of inoculation, $n = 1$.

4. Discussion

Using gravity, wood cell orientation, and directional colonization, our wafer design worked well for partitioning fungal metabolites and wood modifications from the hyphal elongation zone to an area of older, perhaps autolysing hyphae. In this fashion, the spatial gradient can be applied to temporal dynamics *in planta* without introducing the variability inherent when harvesting from replicate wafers and microcosms. Our design also provided resolution in single-mm sections of intact wood, giving 40× higher resolution than the packed-column approach of Hahn et al. (2012) using 4-cm sections of colonized sawdust. This resolution is important in our case of probing extracellular mechanisms, given that our zone of interest for a follow-up study would be less than a 1-cm distance in the wafer.

Inside wood, hyphae were commonly seen moving cell-to-cell by penetrating bordered pits. Isolated hyphae ahead of the obvious hyphal front may either be exploratory within the wood or colonizers from the wood surface, and these may be responsible for slight variability in EG activity, as is apparent around 58 mm in Fig. 3B. This suggests that activity might be related to the amount of active fungal biomass at a given location, more than gene upregulation, and this fits observations of constitutive cellulase production for brown rot fungi (Highley, 1973; Cotoras and Agosin, 1992). In any case, it further supports the need to maintain directional growth if a temporal series is the goal, as well as to extrapolate from solid wood where colonization is from cell-to-cell and fungal expression is within its natural environmental context.

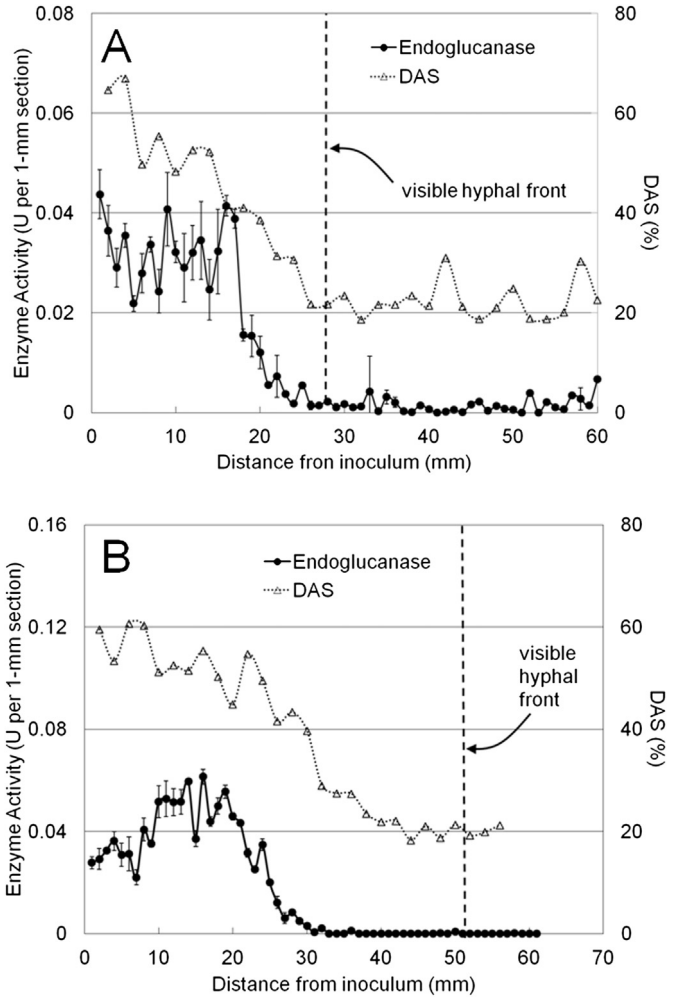

Fig. 5. Colocalization in wood wafers colonized by *P. placenta* of endoglucanase with dilute alkali solubility (DAS), a proxy for carbohydrate depolymerization. Shown are two wafers one from day 14 (A) and the other from day 18 (B), with well-developed and abrupt EG fronts and a typical increase in DAS to that of non-colonized wood, coincident with the EG front. Error bars are standard deviations.

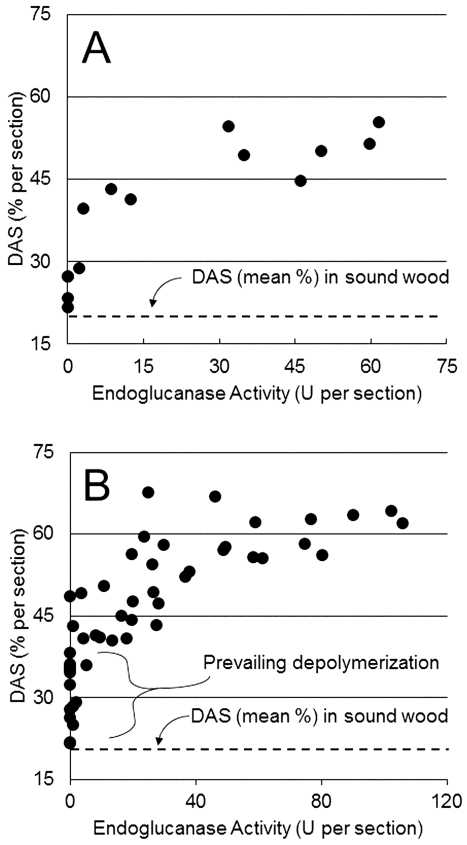

Fig. 6. Correlation of alkali solubility with EG activity per section of wood wafers, showing a zone of depolymerization (6–8 mm) in front of detectable EG (and, by default, demethylation; see Fig. 4). A less-developed 18-day wafer (A) and data pooled from three more developed 3-week wafers (B) are shown. Because DAS was performed every 2 mm, while EG every 1 mm, only coincident data was used and the progression was thus at 2-mm increments.

Detection of EG activity and of oxidative tissue modifications lagged behind the hyphal front as well as the acidification of wafers, but were coincident with each other. For pH, there may be a moisture differential barring diffusion ahead of the hyphal front, but acidification to low pH typical of brown rot (Green et al., 1991; Schilling and Jellison, 2005) was evident behind the hyphal front and ahead of the EG front. Tissue modifications predicted to relate to oxidative Fenton-based chemistry were generally coincident with the EG front, not preceding them. Unequal detection limits for EG activity versus lignin demethylation could show coincident fronts artificially, but in this sampling design, results from one are coupled to the other. Data were pooled relative to the EG front and from wafers with varying EG activity (different *y*-axis amplitudes) at the front. With fourteen replicate wafers, this makes false coincident fronts seem unlikely, although we cannot rule out the possibility that lignin measures were reliably less sensitive (with precision) than the EG activity assay. If, on the other hand, enzymatic cellulolysis and oxygen radical reactions with lignin are truly coincident and not partitioned over large distances, it would be useful to know how these two incompatible reactions overlap at discrete locations. Perhaps high levels of protective glycosylation (Clausen, 1995) or an inability to diffuse into the wood cell wall (Fluornoy et al., 1991; Srebotnik and Messner, 1991) protect the enzyme from oxidative stress, the former as coincident reactions and the latter partitioned. There is also the possibility that lignin modifications measured do not reflect the action of reactive oxygen species. In any case, it would be useful to resolve these reactions at a finer scale per individual wood cells ($\sim$<30 μm).

Surprisingly, an increase in depolymerization was detectable well ahead of the coincident oxidative and enzymatic proxies. DAS correlation with EG activity in Fig. 6A and B shows depolymerization without detectable EG for 6–8 mm of wood wafer, a significant distance given the size of our wafers. Although the same caveat regarding detection limits applies, there are several explanations to consider that might inform more targeted follow-up trials. One explanation is that some component of the theorized reaction partitioning sequence does not occur for *P. placenta* as hypothesized. As mentioned, lignin modifications might simply be a side effect not related carbohydrate depolymerization mechanisms. Lignin modifications induced by brown rot fungi, however, are distinct to those of white rot (Filley, 2003), and *P. placenta* has commonly been shown to struggle in depolymerizing crystalline cellulose without lignin present (Highley, 1980; Enoki et al., 1988). Another explanation could be that depolymerization is initiated by other means, perhaps acid-hydrolysis or cellulolytic enzymes not measured here. Concerning acidification, the DAS correlates well with the drop in pH behind the hyphal front, and it is well known that wood carbohydrates are easily depolymerized by acid-hydrolysis. Historically, however (e.g., Koenigs, 1974), the dissimilarity in DAS between simple acid-hydrolysis and brown rot in wood has been used to discount a direct relationship between pH and depolymerization. Concerning

enzymes, poorly-researched candidates such as GH61 family polysaccharide monooxygenases (PMOs) are increasingly implicated in a cellulolytic arsenal that, to date, has likely been over-simplified (Žifčáková and Baldrian, 2012). For *P. placenta*, however, these particular genes are not upregulated when in wood contact as they are among white rot fungi, and this would not explain the inefficiency of crude *P. placenta* extracts saccharifying crystalline cellulose substrates (e.g., filter paper) (Wymelenberg et al., 2010). In short, the secretome of brown rot fungi and its modes of action in lignocellulose remain poorly understood, and our wafer design and its results can better target this inquiry.

The wafer construct has the maximum effect in segregating reactions zones *in planta*, somewhat like chromatography, with a shorter development period (2–3 weeks) than traditional whole-block trials (2–3 months). There is a growing array of molecular and imaging tools available to those studying the lignocellulolytic mechanisms of filamentous fungi, but these tools must be applied with better spatiotemporal resolution than a whole-block approach can provide. To this end, visual placement of the hyphal front in our wafers can help predict progress within wood cells, and this can, in turn, target small-scale efforts in areas of incipient depolymerization. This can include mapping gene expression spatially and then correlating both the observed secretome and chemical changes in the lignocellulose. Often, researchers implicate connections between substrate modifications and the metabolites presumed responsible, without being able to verify this link between cause and effect. This design may strengthen or refute such links, harnessing a spatial gradient to tell a temporally-resolved story of how a brown rot fungus unlocks energy from wood.

Acknowledgements

This work was made possible by US Department of Energy (DOE) grants GO18088 from the Biomass Research and Development Initiative (BRDI) and DE SC0004012 Early Career from the Biological and Ecological Research (BER) program, along with an Early Career grant (RC 008-11) from the Initiative for Renewable Energy and the Environment (IREE), a program of the Institute on the Environment (IonE) at the University of Minnesota. The authors would like to thank Dr. Charles Abbas from Archer Daniels Midland (ADM) Company and Mr. Justin Kaffenberger for technical input, along with Mr. Benjamin Held for his help in confocal image retrieval and interpretation.

References

ASTM, 2007. Standard Test Method for 1% Sodium Hydroxide Solubility of Wood. ASTM International, West Conshohocken, PA. Standard D1109 – 84.

Campbell, W.G., 1952. The biological decomposition of wood. In: Wise, L.E., Jahn, E.C. (Eds.), 1952. Wood Chemistry, vol. 2. Rheinhold Pub. Corp., N.Y., pp. 1061–1116.

Clausen, C.A., 1995. Dissociation of the multi-enzyme complex of the brown-rot fungus *Postia placenta*. FEMS Microbiology Letters 127, 73–78.

Cotoras, M., Agosin, E., 1992. Regulatory aspects of endoglucanase production by the brown-rot fungus Gloeophyllum trabeum. Experimental Microbiology 16, 253–260.

Cowling, E.B., 1961. Comparative Biochemistry of the Decay of Sweetgum Sapwood by White-rot and Brown-rot Fungi. In: U.S. Department of Agriculture, Technical Bulletin, vol. 1258.

Curling, S.F., Clausen, C.A., Winandy, J.E., 2002. Relationships between mechanical properties, weight loss, and chemical composition of wood during incipient brown-rot decay. Forest Products Journal 52, 34–39.

Eastwood, D.C., Floudas, D., Binder, M., Majcherczyk, A., Schneider, P., Aerts, A., Asiegbu, F.O., Baker, S.E., Barry, K., Bendiksby, M., Blumentritt, M., Coutinho, P.M., Cullen, D., de Vries, R.P., Gathman, A., Goodell, B., Henrissat, B., Ihrmark, K., Kauserud, H., Kohler, A., LaButti, K., Lapidus, A., Lavin, J.L., Lee, Y.H., Lindquist, E., Lilly, W., Lucas, S., Morin, E., Murat, C., Oguiza, J.A., Park, J., Pisabarro, A.G., Riley, R., Rosling, A., Salamov, A., Schmidt, O., Schmutz, J., Skrede, I., Stenlid, J., Wiebenga, A., Xie, X., Kües, U., Hibbett, D.S., Hoffmeister, D., Högberg, N., Martin, F., Grigoriev, I.V., Watkinson, S.C., 2011. The plant cell wall-decomposing machinery underlies the functional diversity of forest fungi. Science 333, 762–765.

Enoki, A., Tanaka, H., Fuse, G., 1988. Degradation of lignin-related compounds, pure cellulose, and wood components by white-rot and brown-rot fungi. Holzforschung 42, 85–93.

Eriksson, K., Blanchette, R.A., Ander, P., 1990. Microbial and Enzymatic Degradation of Wood and Wood Components. Springer, Berlin.

Espejo, E., Agosin, E., 1991. Production and degradation of oxalic acid by brown rot fungi. Applied and Environmental Microbiology 57, 1980–1986.

Filley, T.R., 2003. Assessment of fungal wood decay by lignin analysis using tetramethyl-ammonium hydroxide (TMAH) and C-13-labeled TMAH thermochemolysis. In: Goodell, B., Nicholas, D.D., Schultz, T.P. (Eds.), Wood Deterioration and Preservation-advances in Our Changing World, ACS Symposium Series, pp. 119–139.

Filley, T.R., Cody, G.D., Goodell, B., Jellison, J., Noser, C., Ostrofsky, A., 2002. Lignin demethylation and polysaccharide decomposition in spruce sapwood degraded by brown rot fungi. Organic Geochemistry 33, 111–124.

Filley, T.R., Wang, Y., Nierop, K.G.L., 2006. The contribution of polyhydroxyl aromatic compounds to tetramethylammonium hydroxide lignin-based proxies. Organic Geochemistry 36, 711–727.

Floudas, D., Binder, M., Riley, R., Barry, K., Blanchette, R.A., Henrissat, B., Martinez, A.T., Otillar, R., Spatafora, J.W., Yadav, J.S., Aerts, A., Benoit, I., Boyd, A., Carlson, A., Copeland, A., Coutinho, P.M., de Vries, R.P., Ferreira, P., Findley, K., Foster, B., Gaskell, J., Glotzer, D., Gorecki, P., Heitman, J., Hesse, C., Hori, C., Igarashi, K., Jurgens, J.A., Kallen, N., Kersten, P., Kohler, A., Kues, U., Kumar, T.K.A., Kuo, A., LaButti, K., Larrondo, L.F., Lindquist, E., Ling, A., Lombard, V., Lucas, S., Lundell, T., Martin, R., McLaughlin, D.J., Morgenstern, I., Morin, E., Murat, C., Nagy, L.G., Nolan, M., Ohm, R.A., Patyshakuliyeva, A., Rokas, A., Ruiz-Duenas, F.J., Sabat, G., Salamov, A., Samejima, M., Schmutz, J., Slot, J.C., St. John, F., Stenlid, J., Sun, H., Sun, S., Syed, K., Tsang, A., Wiebenga, A., Young, D., Pisabarro, A., Eastwood, D.C., Martin, F., Cullen, D., Grigoriev, I.V., Hibbett, D.S., 2012. The Paleozoic origin of enzymatic lignin decomposition reconstructed from 31 fungal genomes. Science 336, 1715–1719.

Fluornoy, D.S., Kirk, T.K., Highley, T.L., 1991. Wood decay by brown-rot fungi: changes in pore structure and cell wall volume. Holzforschung 45, 383–388.

Gilbertson, R., 1980. Wood-rotting fungi of North America. Mycologia 72, 1–49.

Gilbertson, R.L., Ryvarden, L., 1986. North American Polypores, vol. 1. Fungiflora, Oslo.

Goodell, B., Jellison, J., Liu, J., Daniel, G., Paszczynski, A., Fekete, F., Krishnamurthy, S., Jun, L., Xu, G., 1997. Low molecular weight chelators and phenolic compounds isolated from wood decay fungi and their role in the fungal biodegradation of wood. Journal of Biotechnology 53, 133–162.

Green III, F., Larsen, M.J., Winandy, J.E., Highley, T.L., 1991. Role of oxalic acid in incipient brown-rot decay. Material und Organismen 26, 191–213.

Hahn, F., Ullrich, R., Hofrichter, M., Liers, C., 2012. Experimental approach to follow the spatiotemporal wood degradation in fungal microcosms. Biotechnology Journal 8, 127–132.

Highley, T.L., 1973. Influence of carbon source on cellulase activity of white-rot and brown-rot fungi. Wood and Fiber 5, 50–58.

Highley, T.L., 1980. Cellulose degradation by cellulose-clearing and non-cellulose clearing brown-rot fungi. Applied and Environmental Microbiology 40, 1145–1147.

Hyde, S.M., Wood, P.M., 1997. A mechanism for production of hydroxyl radicals by the brown-rot fungus *Coniophora puteana*: Fe(III) reduction by cellobiose dehydrogenase and Fe(II) oxidation at a distance from the hyphae. Microbiology 143, 259–266.

Jurgenson, M.F., Larsen, M.J., Harvey, A.E., 1977. Effects of timber harvesting on soil biology. In: Forests for People: A Challenge in World Affairs. Proceedings of the Society of the American Forester, pp. 244–250.

Kerem, Z., Bao, W., Hammel, K., 1998. Rapid polyether cleavage via extracellular one-electron oxidation by a brown-rot basidiomycete. Proceedings of the National Academy of Sciences 95, 10373–10377.

Kirk, T.K., 1975. Effects of a brown-rot fungus, *Lenzites trabea* on lignin in spruce wood. Holzforschung 29, 99–107.

Koenigs, J.W., 1974. Hydrogen peroxide and iron: a proposed system for decomposition of wood by brown-rot basidiomycetes. Wood and Fiber 6, 66–80.

Martinez, D., Challacombe, J., Morgenstern, I., Hibbett, D., Schmoll, M., Kubicek, C.P., Ferreira, P., Ruiz-Duenas, F.J., Martinez, A.T., Kersten, P.J., Hammel, K.E., Gaskell, J.A., Cullen, D., 2009. Genome, transcriptome, and secretome analysis of wood decay fungus *Postia placenta* supports unique mechanisms of lignocellulose conversion. Proceedings of the National Academy of Sciences 106, 1954–1959.

Rypáček, V., Rypáčková, M., 1975. Brown rot of wood as a model for studies of lignocellulose humification. Biologia Plantarum 17, 452–457.

Saha, B.C., 2004. Lignocellulose biodegradation and applications in biotechnology. In: Saha, B.C., Hayashi, K. (Eds.), *Lignocellulose Biodegradation*. American Chemical Society, Washington, pp. 2–34.

Schilling, J.S., Bissonnette, K., 2008. Iron and calcium translocation from pure gypsum and iron-amended gypsum by two brown rot fungi and a white rot fungus. Holzforschung 62, 752–758.

Schilling, J.S., Jellison, J., 2005. Oxalate regulation by two brown rot fungi decaying oxalate amended and non-amended wood. Holzforschung 59, 680–688.

Schilling, J.S., Ai, J., Blanchette, R.A., Duncan, S.M., Filley, T.R., Tschirner, U.W., 2012. Lignocellulose modifications by brown rot fungi and their effects, as pretreatments, on cellulolysis. Bioresource Technology 116, 147–154.

Shortle, W.C., Dudzik, K.R., Smith, K.T., 2010. Development of wood decay in wound-initiated discolored wood of eastern red cedar. Holzforschung 64, 529–536.

Song, Z., Sadowsky, M., Vail, A., Schilling, J.S., 2012. Competition between two wood-degrading fungi with distinct influences on residues. FEMS Microbiology Ecology 79, 109–117.

Srebotnik, E., Messner, K., 1991. Immunoelectron microscopical study of the porosity of brown-rot degraded pine wood. Holzforschung 45, 95–101.
Winandy, J.E., Morrell, J.J., 1993. Relationship between incipient decay, strength, and chemical composition of douglas-fir heartwood. Wood and Fiber Science 25, 278–288.
Wymelenberg, A.V., Gaskell, J., Mozuch, M., Sabat, G., Ralph, J., Skyba, O., Mansfield, S.D., Blanchette, R.A., Martinez, D., Grigoriev, I., Kersten, P.J., Cullen, D., 2010. Comparative transcriptome and secretome analysis of wood decay fungi *Postia placenta* and *Phanerochaete chrysosporium*. Applied and Environmental Microbiology 76, 3599–3610.
Zabel, R., Morrell, J., 1992. Wood Microbiology: Decay and its Prevention. Academic Press, San Diego.
Žifčáková, L., Baldrian, P., 2012. Fungal polysaccharide monooxygenases: new players in the decomposition of cellulose. Fungal Ecology 5, 481–489.